Ultrafast all-optical Nth-order differentiator based on chirped fiber Bragg gratings

Miguel A. Preciado, Víctor García-Muñoz, and Miguel A. Muriel

ETSI Telecomunicación, Universidad Politécnica de Madrid (UPM), 28040 Madrid, Spain.
miguel.preciado@tfo.upm.es, victorgm@tfo.upm.es, muriel@tfo.upm.es

Abstract: In this letter we present a technique for the implementation of Nth-order ultrafast temporal differentiators. This technique is based on two oppositely chirped fiber Bragg gratings in which the grating profile maps the spectral response of the Nth-order differentiator. Examples of 1st, 2nd, and 4th order differentiators are designed and numerically simulated.

OCIS codes: (060.2340) Fiber optics components; (230.1150) All-optical devices; (320.5540) Pulse shaping; (999.9999) Fiber Bragg gratings.

References and Links

1. N. Q. Ngo , S. F. Yu, S. C. Tjin, and C. H. Kam, "A new theoretical basis of higher-derivative optical differentiators," Opt. Commun. **230**, 115−129, (2004).
2. H. J. A. da Silva and J. J. O'Reilly, "Optical pulse modeling with Hermite - Gaussian functions," Opt. Lett. **14**, 526- (1989).
3. R. Slavík, Y. Park, M. Kulishov, R. Morandotti, and J. Azaña, "Ultrafast all-optical differentiators ," Opt. Express **14**, 10699-10707 (2006).
4. N. K. Berger, B. Levit, B. Fischer, M. Kulishov, D. V. Plant, and J. Azaña, " Temporal differentiation of optical signals using a phase-shifted fiber Bragg grating," Opt. Express **15**, 371-381 (2007).
5. Y. Park, R. Slavik, J. Azaña "Ultrafast all-optical first and higher-order differentiators based on interferometers" Opt. Lett. **32**, 710-712 (2007).
6. M. A. Preciado, V. García-Muñoz, and M. A. Muriel "Grating design of oppositely chirped FBGs for pulse shaping," IEEE Photon. Technol. Lett. **10**, 435-437 (2007).
7. A. G. Jepsen, A. E. Johnson, E. S. Maniloff, T. W. Mossberg, M. J. Munroe, and J. N. Sweetser, "Fibre Bragg grating based spectral encoder/decoder for lightwave CDMA," Electron. Lett. **35**, 1096-1097 (1999).
8. I. Littler, M. Rochette, and B. Eggleton, "Adjustable bandwidth dispersionless bandpass FBG optical filter," Opt. Express **13**, 3397-3407 (2005).
9. J. Azaña and M. A. Muriel, ''Real-time optical spectrum analysis based on the time-space duality in chirped fiber gratings,'' IEEE J. Quantum Electron. **36**, 517–527 (2000).
10. J. Azaña and L. R. Chen, "Synthesis of temporal optical waveforms by fiber Bragg gratings: a new approach based on space-to-frequency-to-time mapping ," J. Opt. Soc. Am. B **19**, 2758-2769 (2002).
11. S. Longhi, M. Marano, P. Laporta, O. Svelto, "Propagation, manipulation, and control of picosecond optical pulses at 1.5 μm in fiber Bragg gratings, J. Opt. Soc. Am. B **19**, 2742-2757 (2002).
12. B. Bovard, "Derivation of a matrix describing a rugate dielectric thin film," Appl. Opt. **27,** 1998–2004 (1988).
13. James F. Brennan III and Dwayne L. LaBrake, "Fabrication of chirped fiber bragg gratings of any desired bandwidth using frequency modulation," US patent 6728444 (April 2004).
14. I. C. M. Littler, L. Fu, and B. J. Eggleton, "Effect of group delay ripple on picosecond pulse compression schemes," Appl. Opt. **44**, 4702-4711 (2005).

1. Introduction

An Nth-order optical temporal differentiator is a device that provides the Nth-time derivative of the complex envelope of an arbitrary input optical signal. This operation is performed on optical devices at operation speeds several orders of magnitude over electronics. These devices may find important applications as basic building blocks in ultrahigh-speed all-optical analog–digital signal processing circuits [1]. Moreover, Nth-order differentiators are of immediate interest for generation of Nth-order Hermite-Gaussian (HG) temporal waveform from an input Gaussian pulse, which can be used to synthesize any temporal shape by

#80259 - $15.00 USD Received 20 Feb 2007; revised 16 May 2007; accepted 23 May 2007; published 29 May 2007

superposition [2]. Several schemes have been previously proposed based on integrated-optic transversal filter [1], long-period fiber gratings [3], phase-shifted fiber Bragg grating [4], and two-arm interferometer [5].

In this letter we use a technique for temporal differentiation based on the use of two oppositely chirped fiber Bragg gratings (FBG) [6]. As it can be seen in Fig. 1, the system includes two linearly chirped FBGs connected by an optical circulator. The first, FBG_a, is the spectral shaper, and provides the spectral response for pulse shaping. The second, FBG_b, cancels the dispersion introduced by the first grating. Obviously, the order of the FBGs can be arbitrarily selected.

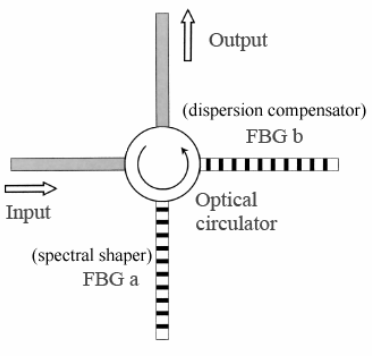

Fig. 1. Architecture of the system. Input signal is processed by two oppositely chirped FBGs, which are connected by an optical circulator.

This scheme has been previously proposed and experimentally demonstrated in [7] and [8]. Specifically, in [7], phase-shifts are introduced in the shaper FBG to generate spectral-phase-encoded bit. In [8], a bandpass Gaussian FBG optical filter in which the bandwidth can be continuously adjusted is presented. Besides the inherent advantages of FBGs (all-fiber approach, low insertion loss, and the potential for low cost), this scheme can provide a direct implementation of an Nth-order differentiator, avoiding the concatenation of N first order differentiators devices. Furthermore, this approach has the possibility of adjusting the bandwidth and tuning the central wavelength [8].

2. Theory

The temporal operation of a Nth-order differentiator can be expressed as $f_{out}(t)=d^N f_{in}(t)/dt^N$, where $f_{in}(t)$ and $f_{out}(t)$ are the complex envelopes of the input and output of the system respectively, and t is the time variable. We can also express this in frequency domain as, $F_{in}(\omega)=(\mathrm{j}\omega)^N F_{out}(\omega)$ where $F_{in}(\omega)$ and $F_{out}(\omega)$ are the spectral functions of $f_{in}(t)$ and $f_{out}(t)$, respectively (ω is the base-band frequency, i.e., $\omega=\omega_{opt}-\omega_0$, where ω_{opt} is the optical frequency, and ω_0 is the central optical frequency of the signals). Thus, the spectral response of the ideal Nth-order differentiator is:

$$F_{out}(\omega) = \left(\mathrm{j}\omega\right)^N F_{in}(\omega)$$

$$H_N(\omega) = F_{out}(\omega)/F_{in}(\omega) \;=\; \left(\mathrm{j}\omega\right)^N \qquad (1)$$

Moreover, in a real system we have a finite bandwidth, so we have to window the spectral response function:

#80259 - $15.00 USD Received 20 Feb 2007; revised 16 May 2007; accepted 23 May 2007; published 29 May 2007

$$H_{N,w}(\omega) = H_N(\omega)W(\omega) \;=\; (\mathrm{j}\omega)^N W(\omega) \tag{2}$$

where $W(\omega)$ is a window function, which must be selected to meet:

$$H_{N,w}(\omega)\begin{cases} \simeq (j\omega)^N & \omega \in \text{ operative band} \\ = trans(\omega) & \omega \in \text{ transient band} \\ \simeq 0 & \omega \notin \text{ band of interest} \end{cases} \tag{3}$$

where the operative band is the region where the differentiator operation works with accuracy, and $trans(\omega)$ is a transient function which must have low amplitude values at the edges of the band of interest in order to avoid an abrupt discontinuity. Notice that not any window function verifies this condition on $trans(\omega)$, even in the case of a window function presenting low values at the edges of the band of interest.

The objective is to obtain a spectral response of the whole system (composed by the two FBGs), $H_{syst}(\omega)$, proportional to the differentiator spectral response:

$$H_{syst}(\omega) = H_a(\omega)H_b(\omega) = \left(R_a(\omega)R_b(\omega)\right)^{1/2} \exp\left(j\left(\phi_a + \phi_b\right)\right) \propto H_{N,w}(\omega) \tag{4}$$

where $H_a(\omega)$, $H_b(\omega)$, $R_a(\omega)$, $R_b(\omega)$, $\phi_a(\omega)$, $\phi_b(\omega)$ are the spectral response in reflection, reflectivity and phase of the FBGs. In this approach we assume that FBG_b is a dispersion compensator, so we can consider that $R_b(\omega)$ presents an ideal flat-top response in the band of interest, so the shape of the reflectivity is influenced by FBG_a solely. Thus, we have:

$$R_a(\omega) \propto \left|H_{syst}(\omega)\right|^2 \propto \left|H_{N,w}(\omega)\right|^2 = \left|\omega^N W(\omega)\right|^2 \tag{5}$$

Regarding the phase, we have two oppositely linearly chirped FBGs, so $\ddot{\phi}_a(\omega) = -\ddot{\phi}_b(\omega) = \ddot{\phi}_a$, where $\ddot{\phi}(\omega)$ denotes $\partial^2\phi(\omega)/\partial\omega^2$, and $\ddot{\phi}_a$ is a constant value, which is obtained from the FBG_a design.

At this point, we present the theory to design the spectral shaper, FBG_a. The refractive index of FBG_a can be written as:

$$n(z) = n_{av,a}(z) + \frac{\Delta n_{\max,a}}{2} A_a(z) \cos\left[\frac{2\pi}{\Lambda_{0,a}} z + \varphi_a(z)\right] \tag{6}$$

where $n_{av,a}(z)$ represents the average refractive index of the propagation mode, $\Delta n_{max,a}$ describes the maximum refractive index modulation, $A_a(z)$ is the normalized apodization function, $\Lambda_{0,a}$ is the fundamental period of the grating, $\varphi_a(z)$ describes the additional phase variation (chirp), and $z \in [-L_a/2, L_a/2]$ is the spatial coordinate over the grating, with L_a the length of FBG_a. In the following we consider a constant average refractive index $n_{av,a}=n_{eff,a}+(\Delta n_{max,a}/2)$, where $n_{eff,a}$ is the effective refractive index of the propagation mode.

Notice that (1) implies that when N is odd, the differentiator spectral response presents a π-phase shift at $\omega=0$. In our approach, this condition is attained by introducing a π-phase shift

#80259 - $15.00 USD Received 20 Feb 2007; revised 16 May 2007; accepted 23 May 2007; published 29 May 2007

in the grating of FBG_a at z=0. The chirp factor of FBG_a, which is defined as $C_{K,a} = \partial^2 \varphi_a(z) / \partial z^2$, and L_a can be calculated from [9]:

$$C_{K,a} = -4n_{av,a}^2 / (c^2 \ddot{\phi}_a) \tag{7}$$

$$L_a = \left|\ddot{\phi}_a\right| c\Delta\omega_{g,a} \Big/ \left(2n_{av,a}\right) \tag{8}$$

where c is the light vacuum speed, and $\Delta\omega_{g,a}$ is the FBG_a bandwidth. It is well known that when a chirped FBG introduces an enough high dispersion, the spectral response of the grating is a scaled version of its corresponding apodization profile [10]. This high dispersion condition can be expressed as:

$$\left|\ddot{\phi}_a\right| >> \left(\Delta t_a\right)^2 / 8\pi \tag{9}$$

where Δt_a is the temporal length of the inverse Fourier transform of the FBG_a spectral response without the dispersive term, which can be calculated from the temporal length of $\Im^{-1}\left[H_{N,w}(\omega)\right]$, where $\Im^{-1}$ denotes inverse Fourier transform. It is worth noting that the broader (narrower) bandwidth, the shorter (longer) minimum length of the grating required for FBG_a to map properly the spatial profile on the spectral response [6].

If condition (9) is met and Born approximation is applicable, both temporal and spectral envelopes reproduce the shape of the apodization profile function, so we can obtain the apodization profile which corresponds to $R_a(\omega)$ [11]. In the case of high reflectivity an approximate function [12] must be applied over $R_a(\omega)$. In particular, a logarithmic based function is used in our approach, and we obtain an expression which is valid for both weak and strong gratings:

$$A_a(z) = \left[-\ln\left(1 - R_a(\omega)\Big|_{\left(\omega = sign\left(C_{K,a}\right)\frac{\Delta\omega_{g,a}}{L_a} z\right)}\right) \frac{32 n_{av,a}^2}{\pi\omega_0^2 \left|\ddot{\phi}_a\right| \Delta n_{\max,a}^2} \right]^{\frac{1}{2}} \tag{10}$$

3. Examples and results

Here we give three design examples for 1st, 2nd and 4th order differentiators, which are numerically simulated. For all the examples we assume a carrier frequency ($\omega_0/2\pi$) of 193 THz, an effective refractive index $n_{eff,a}$=1.45 for FBG_a, a band of interest ($\Delta\omega/2\pi$) of 5 THz centred at ω_0 (ω_0-$\Delta\omega/2 \le \omega_{opt} \le \omega_0$+$\Delta\omega/2$), a FBG_a bandwidth $\Delta\omega_{g,a}$=$\Delta\omega$, and a maximum reflectivity for FBG_a of 90 %.

In the first example we design a system which implements a 1st-order differentiator. The corresponding ideal spectral response is $H_1(\omega)$=jω, and we choose a function based on a hyperbolic tangent as window, $W_{th}(\omega)$=(1/2)[1+tanh(4-|16$\omega/\Delta\omega$|)]:

$$H_{syst}(\omega) \propto H_{1,w}(\omega) = H_1(\omega) W_{th}(\omega) = \begin{cases} \dfrac{\mathrm{j}\omega}{2}\left[1+\tanh\left(4-\left|16\dfrac{\omega}{\Delta\omega}\right|\right)\right] & |\omega| \le \dfrac{\Delta\omega}{2} \\ 0 & |\omega| > \dfrac{\Delta\omega}{2} \end{cases} \tag{11}$$

#80259 - $15.00 USD Received 20 Feb 2007; revised 16 May 2007; accepted 23 May 2007; published 29 May 2007

The spectral shaper (FBG_a) must be designed to properly map the desired spectral response. From the temporal length of $\Im^{-1}\left[H_{1,w}(\omega)\right]$ we obtain $\Delta t_a \approx 2$ ps. Using expression (9) we have $\left|\ddot{\phi}_a\right| >> 1.5915\times10^{-25}\, s^2/rad$, and choose $\ddot{\phi}_a = -1.6\times10^{-23}\, s^2/rad$. Moreover, the odd order of 1st differentiator implies that π-phase shift must be introduced in FBG_a at z=0. The desired reflectivity for FBG_a in the band of interest is obtained from (5):

$$R_a(\omega) = \left\{ C_R\left(\omega/\Delta\omega_{g,a}\right)\left[1+\tanh\left(4-\left|16\omega/\Delta\omega_{g,a}\right|\right)\right] \right\}^2 \tag{12}$$

where C_R=2.8494 is a normalization constant selected to get a maximum reflectivity $\max(R_a(\omega))$=0.9. Using (10) at the maximum reflectivity and apodization, with $\max(A_a(z))$=1, we obtain $\Delta n_{max,a}$=1.4484 x 10^{-3}, $n_{av,a}$=1.45072.

Additionally, using (7) and (8), we obtain $C_{K,a}$=5.8543 x 10^6 rad/m^2 and L_a=5.1936 cm. The fundamental period of the grating FBG_a can be obtained from $\Lambda_{0,a}=\pi c/(n_{av}\omega_0)$=535.36 nm. The period of FBG_a varies from 542.39 nm to 528.51 nm along the length of the grating. This supposes a relative period variation of 2.591 %, which is within accuracy of currently available fabrication techniques [13].

Finally, using (10) we obtain the apodization profile function:

$$A(z) = C_A\left(-\ln\left\{ 1-C_R^{\,2}\left|\frac{z}{L_a}\right|^{2N}\left[1+\tanh\left(4-\left|16\frac{z}{L_a}\right|\right)\right]^2\right\}\right)^{1/2} \tag{13}$$

where C_A=0.659 is a normalization constant selected to get a normalized apodization profile function $0\le A_a(z)\le 1$, and N=1.

Moreover, the dispersion parameter of the dispersion compensator (FBG_b) is $\ddot{\phi}_b(\omega) = -\ddot{\phi}_a = -1.6\times10^{23}\, s^2/rad$, which must present a flat top spectral response in the band of interest.

As a second example we design a 2nd order differentiator using the same methodology. We obtain again $\Delta t_{g,a}\approx 2$ ps, so we have the same technological parameters as in the first example. The apodization profile which is given by (13), where C_R= 13.568, and N=2 (same L_a and C_A as for first example).

Finally, in a third example, we design a 4th order differentiator. We have again $\Delta t_{g,a}\approx 2$ ps, and the same technological parameters, with an apodization profile described by (13), where C_R= 243.1, and N=4 (same L_a and C_A as for first example).

Figure 2 shows the results from our numerical simulations corresponding to these examples. Figures 2(a), 2(b), and 2(c) show the phase response of the spectral shaper (FBG_a), the dispersion compensator (FBG_b), and the whole system, for the first, second and third example, respectively. Figures 2(d), 2(e), and 2(f) compare the spectral responses of the spectral shaper (FBG_a) and the ideal differentiator, for the first, second and third example, respectively. Figures 2(g), 2(h), and 2(i) show the temporal waveform of the input pulse and the output pulses of the designed system, and the ideal differentiator, for the first, second and third example, respectively. We have applied an input gaussian envelope pulse, described by $f_{in}(t) \propto \exp(-t^2/(2\sigma^2))$, with σ = 500 fs (FWHM= 1.177 ps).

#80259 - $15.00 USD Received 20 Feb 2007; revised 16 May 2007; accepted 23 May 2007; published 29 May 2007

It is worth noting that in our simulations we have supposed ideal cancellation of dispersions of both FBGs. In practice this requires a careful monitoring of the chirp profile of each grating in order to avoid excessive phase ripple. This has been achieved in [7], even with tunable chirp in [8]. Considerations about dispersion and phase ripple tolerance can be found in [8] and [14].

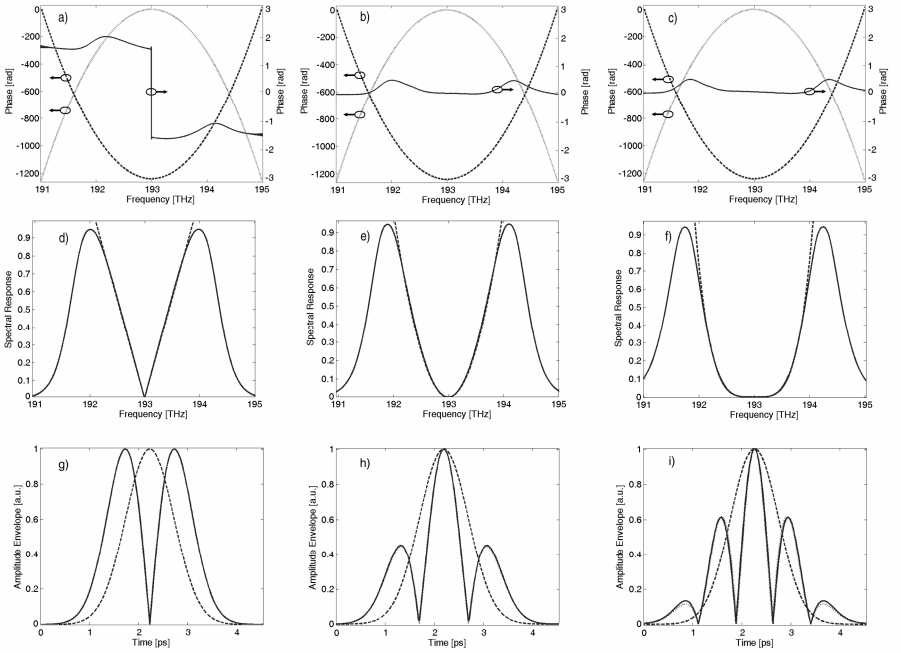

Fig. 2. Plots (a), (b), and (c) show the phase response of the spectral shaper (dotted), the dispersion compensator (dashed), and the whole system (solid). Plots (d), (e), and (f) show the spectral response corresponding to the spectral shaper (solid) for first, second and third example, and to ideal 1st, 2nd, and 4th order differentiator (dashed), respectively. Plots (g), (h), and (i) show the temporal waveforms of the input pulse (dashed), the output pulse corresponding to the system (solid) for first, second and third example, and the output pulse corresponding to ideal 1st, 2nd, and 4th order differentiator (dotted), respectively.

4. Conclusion

In this paper, we have presented an Nth-order differentiator based on a pair of oppositely chirped FBGs, and we have analytically designed and numerically simulated three examples, the 1st, 2nd, and 4th order differentiators.

In addition to the inherent advantages of FBGs, we find two main features that could be of practical relevance. Firstly, we can implement a Nth-order differentiator using a single device, which is more energetically efficient than the concatenation of N first order differentiators. Secondly, the proposed scheme allows tuning the central wavelength and adjusting the bandwidth [8] according to the input signal.

Acknowledgments

This work was supported by the Spanish *Ministerio de Educacion y Ciencia* under Project "Plan Nacional de I+D+I TEC2004-04754-C03-02".

#80259 - $15.00 USD Received 20 Feb 2007; revised 16 May 2007; accepted 23 May 2007; published 29 May 2007